Nuclear Engineering and Design 305 (2016) 666–671

Contents lists available at ScienceDirect

Nuclear Engineering and Design

journal homepage: www.elsevier.com/locate/nucengdes

Effects of thermal aging on microstructure and hardness of China low activation martensitic steel welded joint

Wei Wang [a,b], Junyu Zhang [a,b], Gang Xu [a,*]

[a] Key Laboratory of Neutronics and Radiation Safety, Institute of Nuclear Energy Safety Technology, Chinese Academy of Sciences, Hefei, Anhui 230031, China
[b] University of Science and Technology of China, Hefei, Anhui, China

HIGHLIGHTS

- The hardness of HAZ and WM decreases obviously after aging.
- The precipitation of the Laves-phase in BM is similar to that in HAZ.
- $M_{23}C_6$ particles are conducive to the nucleation of Laves-phase.
- Ta may have a role to retard the early precipitation of the Laves-phase.

ARTICLE INFO

Article history:
Received 24 November 2015
Received in revised form 23 May 2016
Accepted 24 May 2016
Available online 5 July 2016

JEL classification:
B. Materials Engineering

ABSTRACT

The aim of this paper is to investigate the microstructure evolution and the change in hardness distribution of China low activation martensitic steel welded joints after thermal aging at 550 °C for 6000 h. The joint was processed by electron beam welding. Compared to the base metal (BM) and heat affected zone (HAZ), Laves-phase was not formed in weld metal (WM) in the as-aged condition due to the higher tantalum content and less precipitation in WM before aging. The dislocation density decreased in HAZ and WM after aging for 6000 h. The property results showed that hardness of WM and HAZ was decreased significantly after aging for 6000 h due to the weakening of solution strengthening and dislocations strengthening. However, the change in the hardness of the base metal by aging remained at a minor level.

1. Introduction

The reduced activation ferritic/martensitic (RAFM) steels, such as Eurofer97, F82H and CLAM, have been chosen as the primary candidate structural materials for future nuclear fusion reactors because of their better thermo-physical, thermo-mechanical properties and post-irradiation performance compared to the austenitic stainless steels (Huang et al., 2013; Muroga et al., 2002). They are developed based on conventional ferritic/martensitic steels by replacing Nb, Mo and Ni with W, Mn and Ta to avoid long life radioactive isotopes (Lindau et al., 2005).

CLAM steel is developed by Institute of Nuclear Energy Safety Technology, Chinese Academy of Sciences (INEST, CAS), collaborated with many other institutes and universities (Huang et al., 2007, 2011, 2009; Huang and Team, 2014). The CLAM steel has been selected as the primary structural materials in the designs of FDS series PbLi blankets for fusion reactors (Wu, 2007), breeder blanket of China fusion engineering test reactor (CFETR) and China test blanket module for ITER (ITER CN TBM). A series of R&D on CLAM steel, such as welding techniques (Li et al., 2009), properties measurements (Huang et al., 2007, 2009; Wu et al., 2012; Li et al., 2010; Gao et al., 2011), researches on TBM (Wu, 2007; Wu and Team, 2007) and post irradiation performance (Huang et al., 2004), have been conducted.

Welding is an essential procedure in the fabrication of TBM and other important components of the fusion reactor. The welded joints are one of the weakest link and the aging mechanism of the heat affected zone (HAZ) and weld metal (WM) are different from the base metal due to different microstructure. Hence, research on the degradation behavior of the welded joints of CLAM steel after long-term service at high temperature is significant to ensure the safety and stability of the TBM. The microstructure evolution of the joint during thermal aging is more complex than the base metal due to the inhomogeneous microstructure in WM and HAZ. The effect of thermal aging on F82H weldment has been investigated to characterize the microstructure evolution and

* Corresponding author at: No. 350, Shushanhu Road, Hefei, Anhui 230031, China. Fax: +86 551 65593681.
E-mail address: gang.xu@fds.org.cn (G. Xu).

http://dx.doi.org/10.1016/j.nucengdes.2016.05.035
0029-5493/

properties change (Sawai et al., 2000; Alamo et al., 2000). However, very rare researches have been conducted on that of CLAM. This paper focuses on the changes of microstructure and hardness distribution of the electron beam welded joint of CLAM steel after thermal aging for 6000 h.

2. Experimental details

The chemical composition of CLAM steel used in this investigation is listed in Table 1. The specimens were wire cut from hot-rolled CLAM steel plate, following with normalizing at 980 °C for 30 min with air cooling and then tempering at 760 °C for 90 min followed by air cooling. The welded joints of CLAM steel were produced by electron beam welding (EBW) processes without post-welding heat treatment. The welding voltage and current were 55 kV and 60 mA, respectively, at constant welding speed of 10 mm/s. Then, the welded specimens were subjected to exposure at 550 °C up to 6000 h in a tube furnace.

The microstructures of welded specimens before and after aging were analyzed by a scanning electron microscope (SEM; ZEISS ΣIGMA) and a transmission electron microscope (TEM; FEI Tecnai G2 F20 S-TWIN). All specimens used for SEM observation were etched by the reagent with a solution of 5 g $FeCl_3$, 15 mL HCl and 75 mL H_2O. The Ø3 mm discs used for TEM observation were taken from WM, HAZ and BM of the weldments before and after aging. The thickness of discs were polished down to below 0.1 mm, and then, electro-polished to the final thickness with a solution of 10% perchloric acid and 90% ethanol by a twin-jet electro-polisher at temperature of −8 °C and voltage of 40 V.

The Vickers hardness tests of the CLAM steel weldments before and after aging were conducted with a load of 0.03 N and holding time of 10 s. The measurement intervals along welded specimens were 0.3 mm and 0.15 mm in BM and welded joints (HAZ and WM), respectively. More than 200 data of hardness were obtained for each specimen.

3. Results and discussion

3.1. Microstructure

3.1.1. Base metal

The SEM micrographs of BM in the as-welded and as-aged condition are shown in Fig. 1. No evident lath martensite was found in BM, and the precipitates were located along boundaries of the prior austenite grains, as shown in Fig. 1(a). After the long-term aging, the microstructure of BM did not change obviously (Fig. 1(b)).

Fig. 2 illustrates the microstructure and precipitated phases of BM before and after aging with TEM micrographs. The morphologies and EDS analysis of the precipitate in the BM are shown in Fig. 3. Martensitic laths, together with precipitates, were observed in BM in the as-welded condition as shown in Fig. 2(a). The width of the laths was about 0.32 μm. The carbides were discontinuously located along the boundaries of grains and laths, which had two mainly morphologies, rod-shape and ellipsoid-shape. The rod-shape carbides with about 121 nm in length and 45 nm in width were mostly precipitated along the martensitic lath boundaries. The ellipsoid-shape carbides with about 100 nm in length and 61 nm in width were mainly located along the prior austenite grain boundaries. The chemical compositions of the carbides in as-welded condition are presented in Fig. 3(c). It showed that the carbides were Cr-rich phases. According to the previous reports on RAFM steel (Klimenkov et al., 2012; Huang et al., 2013; Shiba et al., 2011; Hu et al., 2013), the Cr-rich phases might be $M_{23}C_6$ ($(Fe, Cr, W)_{23}C_6$ carbides). Moreover, a high dislocation density in the BM before aging was also revealed in Fig. 3(a). After aging for 6000 h, some martensitic laths were decomposed into sub-grains as shown in Fig. 2(b). The sizes of the sub-grain were 0.5–0.8 μm. In the as-aged condition, the carbides were coarsened (Fig. 2(b)), and mainly distributed as a continuous chain along the grain boundaries (Fig. 3(b)). The length and width of the carbide was increased to 133 nm and 100 nm, respectively. Furthermore, a new kind of particle was formed in the BM. The EDS analysis showed that the chemical composition of the new particle was 49Fe–9Cr–42W (in wt.%). Tamura et al. identified that the W-rich particle could be Laves-phase (Tamura et al., 2000). The Laves-phase was precipitated at the grain boundaries associating with $M_{23}C_6$, which would be beneficial for the Laves-phase growth to obtain W element by engulfing the $M_{23}C_6$ carbides and reduce the phase transformation free energy (Hu and G., 2006).

3.1.2. Heat affected zone

The influence of aging on microstructure and precipitation in heat affected zone of CLAM weldments was also investigated by SEM and TEM, as shown in Figs. 4 and 5. In as-welded condition, a few large particles were precipitated along the grain boundaries. The average size of the large particles was about 70 nm. However, much smaller particles with a size of about 20 nm were located within the grain as shown by Fig. 4(a). The particles before aging had two types: ellipsoid-shape $M_{23}C_6$ carbides and spherical-shape TaC as presented in Fig. 5(a). The analysis of EDS indicated that the large particles were Cr-enriched $M_{23}C_6$ carbides and the small particles were Ta-enriched TaC carbides. The results in Fig. 5c shows that the chemical composition of the Ta-rich phase was 6 0Ta–30Fe–4Cr–2C–3V–W (in wt.%). The SEM and TEM images revealed that the microstructure in the fully quenched-tempered zone (FQTZ) was homogeneous and the grain size was even more uniform (Zhu et al., 2014). In the FQTZ, the tempered martensite of the base metal was transformed to the austenite at heat temperature over Ac_3. The particles could not be fully dissolved due to the high heating speed, then the residual particles kept in the matrix during continuous cooling. That was why there were few small particles in the matrix before thermal aging.

After aging for 6000 h, both the number and size of particles increased (Fig. 4(b)). The length and width of $M_{23}C_6$ increased to about 110 nm and 80 nm, respectively. Moreover, the Laves-phase with the chemical composition of 35W–56Fe–9Cr was also observed at the grain boundaries associating with the $M_{23}C_6$ particles, as shown in Fig. 5(b) and (d). The length and width of the Laves-phase was about 200 nm and 25 nm, respectively, which were similar to that in BM. However, the number of particles in HAZ was less than that in BM after the aging process. Fig. 5 also shows that the dislocation density has been decreased during the thermal exposure. It was considered to be the result of the dislocation annihilation caused by dislocation motion at elevated temperature (Cerjak et al., 1999; Panait et al., 2010).

3.1.3. Weld metal

Figs. 6 and 7 are the micrographs of SEM and TEM analysis on microstructure and precipitation of WM in the as-welded and aged condition.

Table 1
Chemical compositions of base metal.

Element	C	Cr	Ta	V	W	Si	Mn	P	S	Fe
wt.%	0.092	8.9	0.14	0.15	1.5	0.05	0.49	0.005	0.002	Bal.

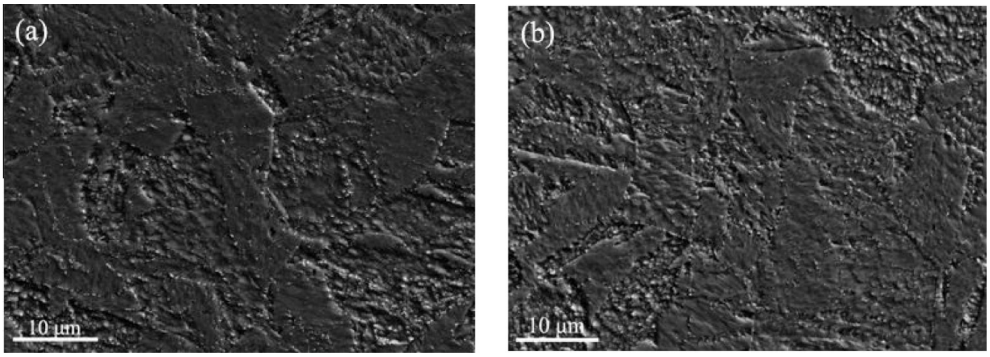

Fig. 1. The SEM images of BM: (a) as-welded; (b) aged 6000 h.

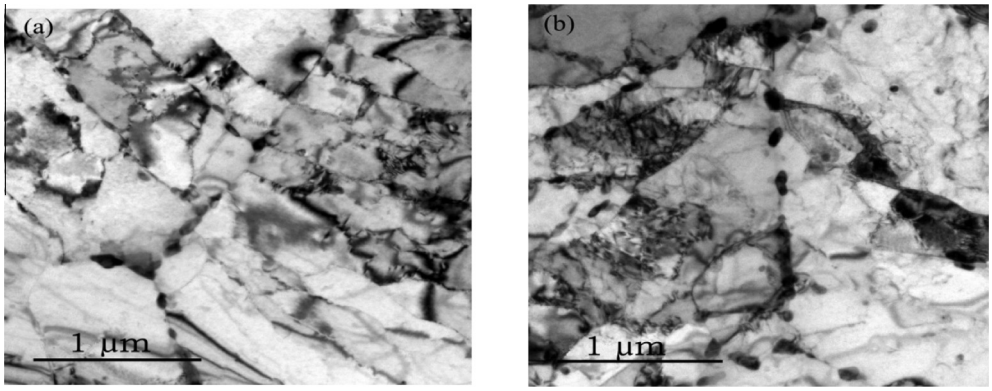

Fig. 2. The TEM images of in BM: (a) as-welded; (b) aged 6000 h.

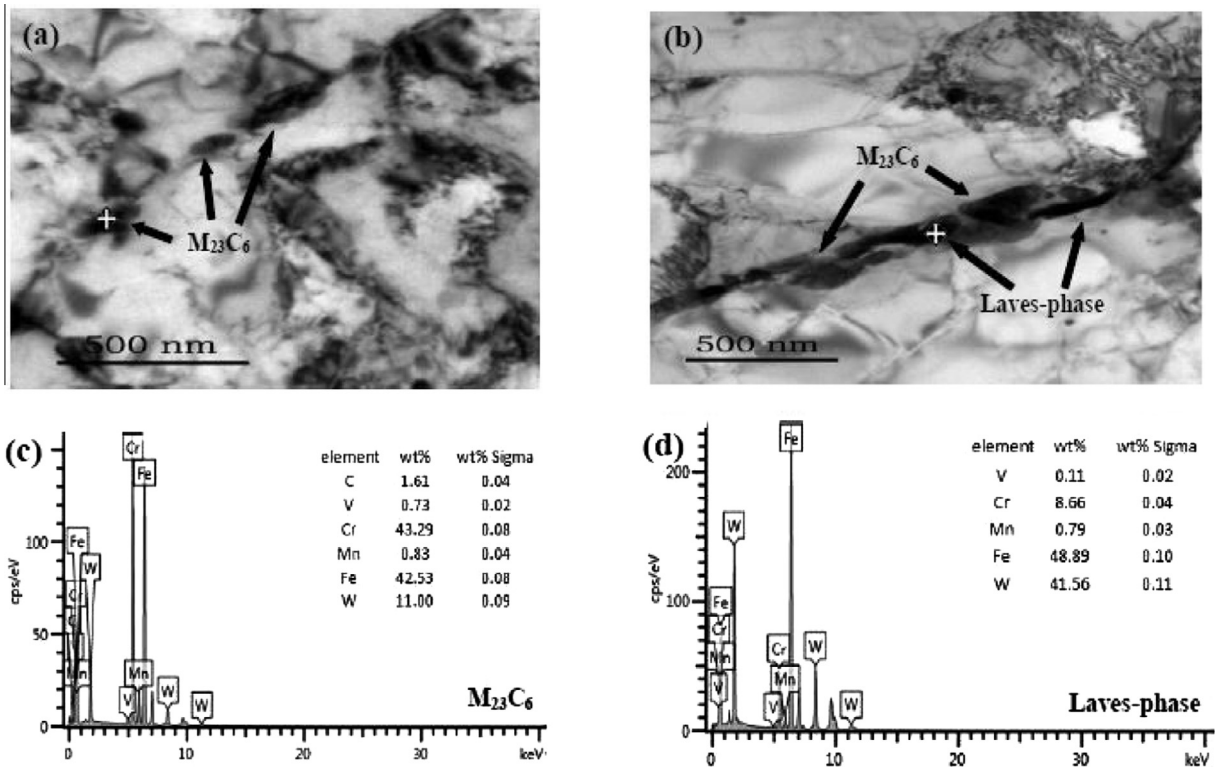

Fig. 3. Precipitates in BM: TEM images of (a) as-welded and (b) 6000 h; EDS analysis of (c) $M_{23}C_6$ and (d) Laves-phase.

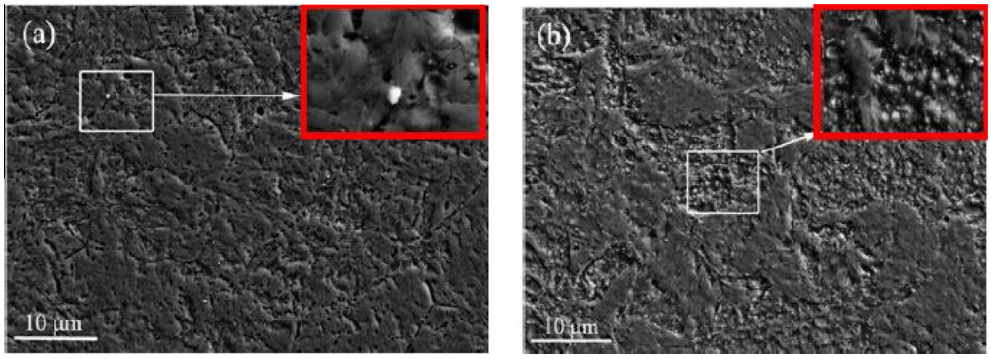

Fig. 4. The SEM images of HAZ: (a) as-welded; (b) aged 6000 h.

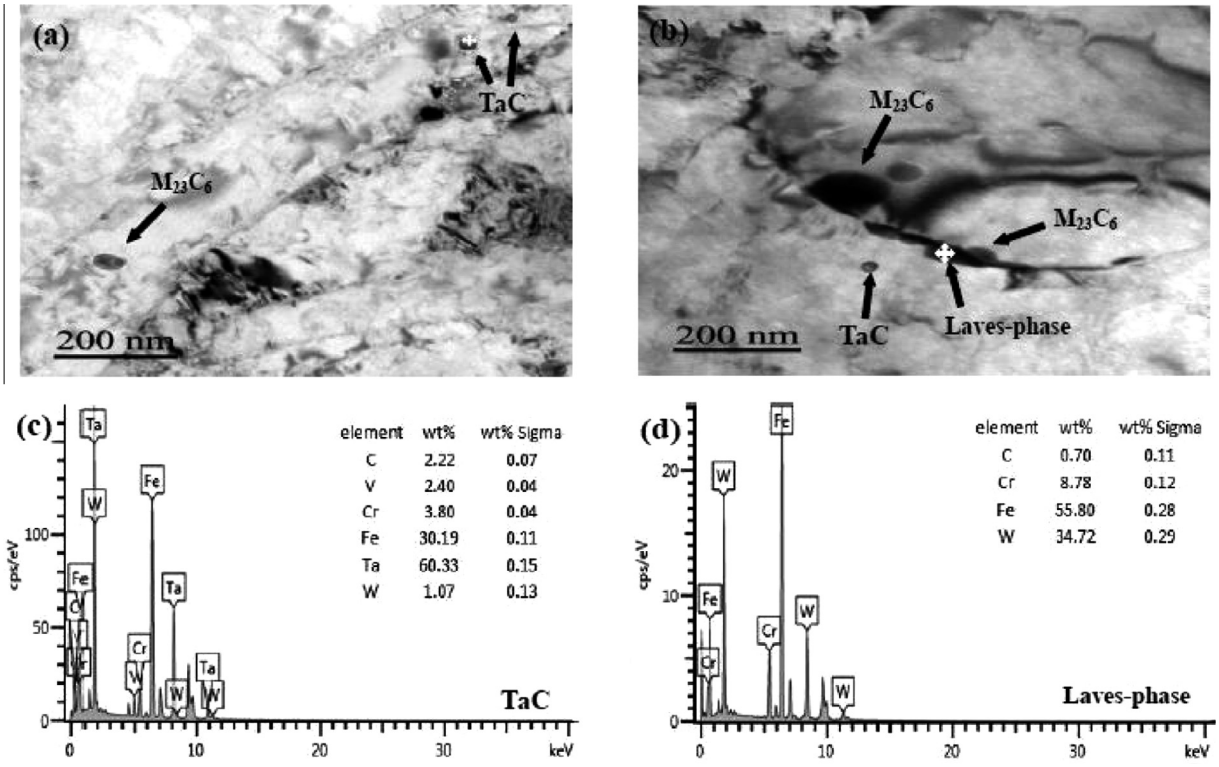

Fig. 5. Precipitates in HAZ: TEM images of (a) as-welded and (b) 6000 h; EDS analysis of (c) TaC and (d) Laves-phase.

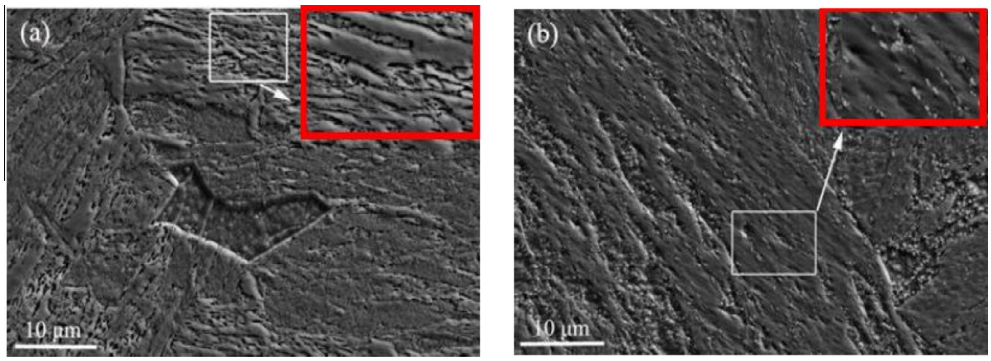

Fig. 6. The SEM images of CLAM steel weldment in WM: (a) as-welded; (b) aged 6000 h.

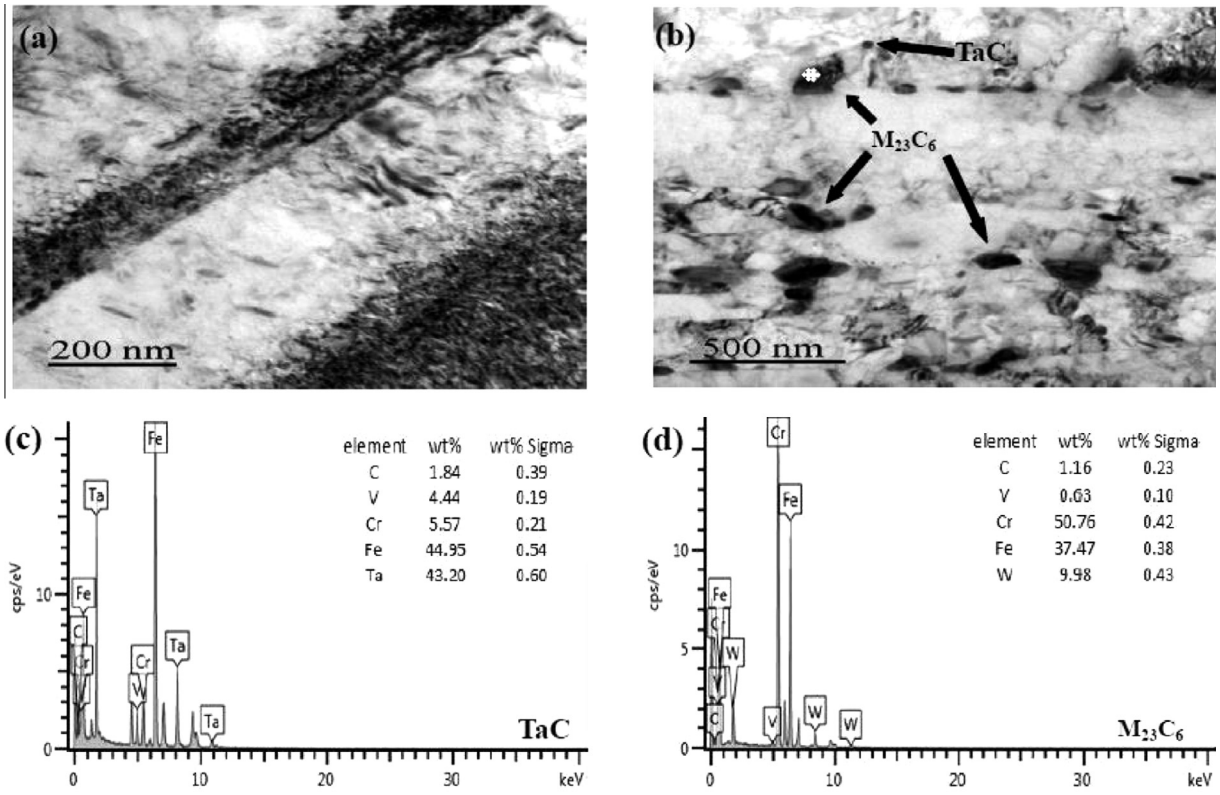

Fig. 7. Precipitates in WM: TEM images of (a) as-welded and (b) 6000 h; EDS analysis of (c) TaC and (d) $M_{23}C_6$.

In the as-welded condition, martensitic laths were observed clearly in Fig. 6(a). The width of the martensitic lath was ranged from 0.8 μm to 1.0 μm. Not any precipitations were found in WM. It also could be seen that the delta ferrite (δ-Fe) was formed in WM. The substructure of the martensitic lath contained high density of dislocations as seen in Fig. 7(a), they were mainly formed during the welding process. After aging for 6000 h, the width of the martensitic lath was increased significantly by 1.4 μm. The reason was that a few precipitations appeared in WM before aging to pin the martensitic lath boundaries and retard the lath coarsening. Nevertheless, the rod-shape particles were precipitated along the prior austenite grain boundaries and martensitic lath boundaries after aging (Fig. 6(b)). The EDS analysis of the precipitations is shown in Fig. 7(c) and (d). The results indicated that the precipitations were Cr-enriched $M_{23}C_6$ and Ta-enriched TaC. The length and width of the rod-shape $M_{23}C_6$ was about 230 nm and 100 nm, respectively. Compared to BM and HAZ, Laves-phase was not found in WM even aging for 6000 h, which was different from other literatures (Sawai et al., 2000). It has reported that Ta might have a role to retard the early precipitation of the Laves-phase (Tamura et al., 1988). In as-welded condition, all elements were dissolved in WM, and the content of Ta in the matrix in WM was higher than that in BM and HAZ. Additionally, $M_{23}C_6$ carbides were conducive to the nucleation of Laves-phase. Compared to BM and HAZ, the formation energy of Laves-phase was higher in WM, and the diffusion of elements to form the Laves-phase needed more time due to the lack of W-rich regions in WM, such as $(Fe, Cr, W)_{23}C_6$ carbides. Hence, no Laves-phase was observed in WM.

3.2. Hardness properties

The hardness profile across the EB welded joint of as-welded and as-aged samples is given in Fig. 8. It showed that the maximum hardness values were observed around the fusion line in both as-welded and aged condition, the values were about 420 HV0.3 and 308 HV0.3, respectively. The hardness distribution in HAZ was gradually decreased from the fusion line to BM. This phenomenon was more obvious in the as-aged sample. However, the hardness fluctuated in WM due to the inhomogeneous microstructure.

After aging for 6000 h, the hardness of HAZ and WM decreased. The reason could be the weakening of solution strengthening and dislocations strengthening. In WM, the nucleation and growth of $M_{23}C_6$ and TaC would reduce the content of alloy elements such as Cr, Ta in matrix. The effect of alloy elements on solid solution strengthening was weakened. The dislocation density also

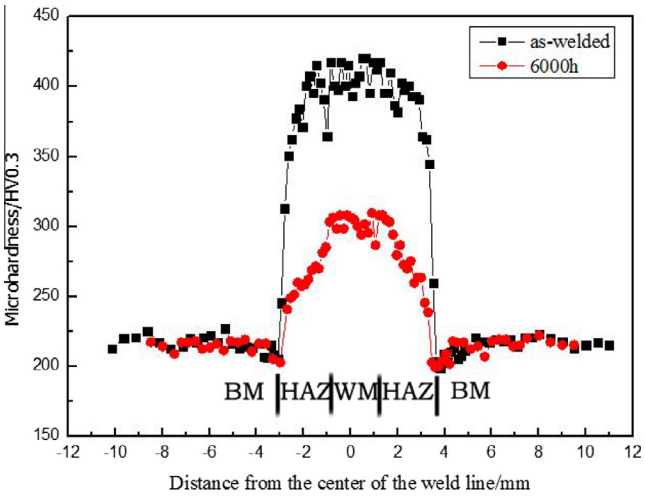

Fig. 8. Effect of aging on hardness distribution along the welded joint.

decreased significantly after aging which would weaken dislocations strengthening. The effects of the two kinds of softening mechanism were stronger than precipitation strengthening by $M_{23}C_6$ and TaC. Those would result in the decreasing of hardness. The reasons of the softening in HAZ were similar to those in WM. However, due to the higher growing speed of Laves-phase and the coarsening of $M_{23}C_6$, the effects of particles on precipitation strengthening in HAZ were weaker than those in WM. So the softening was more obvious in HAZ.

The hardness of base metal in welded condition was about 220 HV0.3 and the change of it was small after aging at 550 °C for 6000 h. The coarsening of $M_{23}C_6$ and formation of Laves-phase would consume the alloy elements in matrix, and then result in weakening of solution strengthening. However, the formation of sub-grain in BM could lead to fine-grain strengthening to counteracting the weakening of solution strengthening.

4. Conclusion

The microstructure and hardness of CLAM weldments in the as-welded and as-aged conditions were investigated in this paper. The main conclusions could be drawn as follows:

(1) In BM, some martensitic laths were decomposed into sub-grains and the $M_{23}C_6$ carbides were coarsened after aging for 6000 h. Laves-phase was precipitated at the grain boundaries associating with $M_{23}C_6$ carbides. However, the change of micro-hardness was negligible even after aging for 6000 h.
(2) In HAZ, a few large particles were found in the as-weld condition. After thermal exposure, both the number and size of particles were increased. The size of Laves-phase in HAZ was smaller than that in BM.
(3) In WM, martensitic laths without precipitation were observed in the as-welded condition. After aging for 6000 h, the $M_{23}C_6$ and TaC were precipitated. Laves-phase was not found in WM after aging. The micro-hardness was decreased significantly after aging with the precipitating of the carbides.

Acknowledgements

This work was supported by the National Magnetic Confinement Fusion Science Program of China with Grant Nos. 2013GB108005 and 2014GB112003. The authors give thanks to Prof. Yican Wu for the guidance on this work and show great appreciation to other members in FDS Team for their support and contribution to this research.

References

Alamo, A., Castaing, A., Fontes, A., Widент, P., 2000. Effects of thermal aging on the mechanical behavior of F82H weldments. J. Nucl. Mater. 283–287, 1192–1195.
Cerjak, H., Hofer, P., Schaffernak, B., 1999. Influence of microstructural aspects on the service behavior of advanced power plant steel. ISIJ Int. 39, 874–888.
Gao, S., Huang, Q., Zhu, Z., Guo, Z., Ling, X., Chen, Y., 2011. Corrosion behavior of CLAM steel in static and flowing LiPb at 480 °C and 550 °C. Fusion Eng. Des. 86, 2627–2631.
Hu, G., Cai, X., Rong, Y., 2006. Foundation of Materials Science, second ed. Shanghai Jiao Tong University Press, Shanghai, China, Ch. 5.
Hu, X., Huang, L., Yan, W., Wang, W., Sha, W., Shan, Y., Yang, K., 2013. Evolution of microstructure and changes of mechanical properties of CLAM steel after long-term aging. Mater. Sci. Eng. A 586, 253–258.
Huang, Q., Team, F.D.S., 2014. Development status of CLAM steel for fusion application. J. Nucl. Mater. 445, 649–654.
Huang, Q., Li, J., Chen, Y., 2004. Study of irradiation effects in china low activation martensitic steel CLAM. J. Nucl. Mater. 329, 268–272.
Huang, Q., Wu, Y., Nagasaka, T., Muroga, T., 2007. Mechanical properties and microstructures of China low activation martensitic steel compared with JLF-1. J. Nucl. Mater. 367–370, 117–121.
Huang, Q., Li, C., Li, Y., Chen, M., Zhang, M., Peng, L., Zhu, Z., Song, Y., Gao, S., 2007. Progress in development of China low activation martensitic steel for fusion application. J. Nucl. Mater. 267–370, 142–146.
Huang, Q., Gao, S., Zhu, Z., Zhang, M., Song, Y., Li, C., Chen, Y., Ling, X., Zhou, X., 2009. Progress in compatibility experiments on lithium-lead with candidate structural material for fusion in China. Fusion Eng. Des. 84, 242–246.
Huang, Q., Wu, Y., Li, J., Wan, F., Chen, J., Luo, G., Liu, X., Chen, J., Xu, Z., Zhou, X., Ju, X., Shan, Y., Yu, J., Zhu, S., Zhang, P., Yang, J., Chen, X., Dong, S., 2009. Status and strategy of fusion materials development in China. J. Nucl. Mater. 386–388, 400–404.
Huang, Q., Li, C., Wu, Q., Liu, S., Gao, S., Guo, Z., Yan, Z., Huang, B., Song, Y., Zhu, Z., Chen, Y., Ling, X., Wu, Y., Team, F.D.S., 2011. Progress in development of CLAM steel and fabrication of small TBM in China. J. Nucl. Mater. 417, 85–88.
Huang, Q., Baluc, N., Dai, Y., Jitsukawa, S., Kimura, A., Konys, J., Kurtz, R.J., Lindau, R., Muroga, T., Odette, G.R., Raj, B., Stoller, R.E., Tan, L., Tanigawa, H., Tavassolo, A., Yamaoto, T., Wan, F., Wu, Y., 2013. Recent progress of R&D activities on reduced activation ferritic/martensitic steels. J. Nucl. Mater. 442, S2–S8.
Huang, L., Hu, X., Yang, C., Yan, W., Xiao, F., Shan, Y., Yang, K., 2013. Influence of thermal aging on microstructure and mechanical properties of CLAM steel. J. Nucl. Mater. 443, 479–483.
Klimenkov, M., Lindau, R., Materna-Morris, E., Möslang, A., 2012. TEM characterization of precipitates in EUROFER 97. Prog. Nucl. Energy 57, 8–13.
Li, C., Huang, Q., Wu, Q., Liu, S., Lei, Y., Muroga, T., Nagasaka, T., Zhang, J., Li, J., 2009. Welding techniques development of CLAM steel for test blanket module. Fusion Eng. Des. 84, 1184–1187.
Li, Y., Nagasaka, T., Muroga, T., 2010. Long-term thermal stability of reduced activation ferritic/martensitic steel as structural materials of fusion blanket. Plasma Fusion Res. 5, S1036–S1039.
Lindau, R., Möslang, A., Rieth, M., Klimiankou, M., Materna-Morris, E., Tavassoli, A.-A.F., Cayron, C., Lancha, A.-M., Fernandez, P., Baluc, N., Schäublin, R., Diegele, E., Filacchioni, G., Rensman, J.W., Schaaf, B.v.d., Lucon, E., Dietz, W., 2005. Present development status of EUROFER and ODS-EUROFER for application in blanket concepts. Fusion Eng. Des. 75–79, 989–996.
Muroga, T., Gasparotto, M., Zinkle, S.J., 2002. Overview of materials research for fusion reactors. Fusion Eng. Des. 61–62, 13–25.
Panait, C., Bendick, W., Fuchsmann, A., Gourgues-Lorenzon, A.-F., Besson, J., 2010. Study of the microstructure of the grade 91 steel after more than 100,000 h of creep exposure at 600 °C. Int. J. Press. Vessels Pip. 87 (6), 326–335.
Sawai, T., Shiba, K., Hishinuma, A., 2000. Microstructure of welded and thermal-aged low activation steel F82H IEA heat. J. Nucl. Mater. 283–287, 657–661.
Shiba, K., Tanigawa, H., Hirose, T., Sakasegawa, H., Jitsukawa, S., 2011. Long-term properties of reduced activation ferritic/martensitic steels for fusion reactor blanket system. Fusion Eng. Des. 86, 2895–2899.
Tamura, M., Hayakawa, H., Yoshitake, A., Hishinuma, A., Kondo, T., 1988. Phase stability of reduced activation ferritic steel: 8%Cr-2%W-0.2%V-0.04%Ta-Fe. J. Nucl. Mater. 155–157, 620–625.
Tamura, M., Shinozuka, K., Esaka, H., Sugimoto, S., Ishizawa, K., Masamura, K., 2000. Mechanical properties of 8Cr-2WVTa steel aged for 30,000 h. J. Nucl. Mater. 283–287, 667–671.
Wu, Y., 2007. FDS team, conceptual design and testing strategy of a dual functional lithium-lead test blanket module in ITER and EAST. Nucl. Fusion 47 (11), 1533–1539.
Wu, Y., 2007. Design status and development strategy of China liquid lithium-lead blankets and related material technology. J. Nucl. Mater. 367–370, 1410–1415.
Wu, Y., Team, F.D.S., 2007. Design analysis of the China dual-functional lithium lead (DFLL) test blanket module in ITER. Fusion Eng. Des. 82, 1893–1903.
Wu, Y., Huang, Q., Zhu, Z., Gao, S., Song, Y., 2012. R&D of dragon series lithium lead loops for materials and blanket technology testing. Fusion Sci. Technol. 62, 272–275.
Zhu, M., Wang, D., Xuan, F., 2014. Effect of long-term aging on microstructure and local behavior in the heat-affected zone of a Ni-Cr-Mo-V steel welded joint. Mater. Charact. 87, 45–61.